APPLYING AN AUTOMATED CRYSTAL SIZE DISTRIBUTION METHOD TO COMPARE LUNAR AND TERRESTRIAL IMPACT MELTS. Hannah C. O'Brien*[1], Aidan M. McDonald*[1], David C. Burney[1] , Karl A. Cronberger[1] Michael A. Torcivia[1] ,Clive R. Neal[1], Annemarie E. Pickersgill[2]. [1]Civil, Environmental Engineering and Earth Science Department, University of Notre Dame,156 Fitzpatrick Hall Notre Dame, IN 46556.[2]School of Geographical & Earth Sciences, University of Glasgow, Gregory Building, Lilybank Gardens, Glasgow G12 8QQ, U.K. (hobrien5@nd.edu)

Introduction: An examination of both terrestrial and lunar impact melt lithologies to determine similarities of phase in these two bodies is crucial to our understanding of the impact process and products. Conducting Crystal Size Distribution (CSD) analyses allows us to determine if a basalt formed through endogenic or impact processes [1]. It also has the benefit of being an inexpensive and non-destructive analytical method [1]. CSDs quantify mineral size populations present within a thin section, specifically the relationship of crystal size with the number of crystals in a specific size range. This relationship is fundamentally linked with nucleation and growth of mineral phases within a crystallizing body [2].

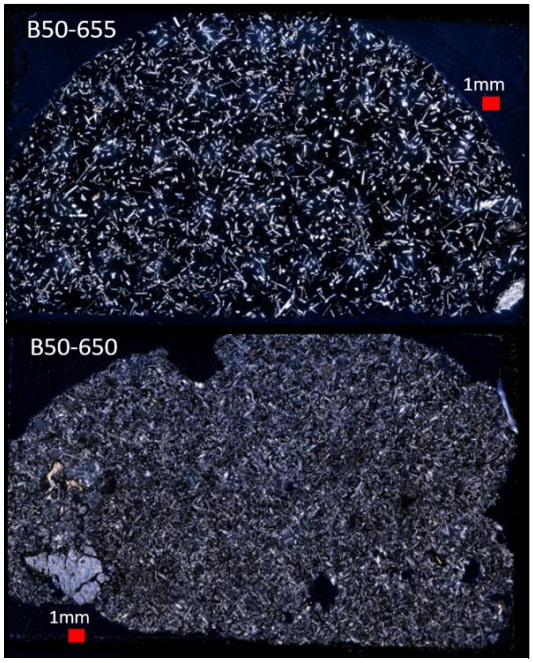

***Figure 1**: Photomosaic of samples B50-655 and B50-650, two of the Boltysh crater samples studied, shown to display petrographic texture.*

Although we have CSD data obtained from lunar basalts, endogenous and impact related, there is a lack of terrestrial impact melt CSDs with which to compare them. This project aims to study these terrestrial impact melts, with impact melt rock samples from the Boltysh impact structure (Ukraine) and other terrestrial samples. A comparison of terrestrial to lunar impact melt CSDs will show similarities or differences between crystallizing melt sheets on the two bodies and may help to provide some additional petrologic context to Apollo impact melt samples.

Samples: Reported here are completed CSDs for impact melt samples from the Boltysh impact structure: B50-650, B50-655, and B50-660 are from the fresh glass section of the B50 drill core, B50-670, B50-675, B50-685 are microcrystalline melt rock from the B50 core, and B1475-774 is from the partially devitrified glass section of drill core B11475 [3]. (**Fig. 1**). Additional CSDs will also be conducted on other terrestrial samples, such as granophyric impact melt rock from the Yarrabubba impact structure, Western Australia (sample YAR-BG1), hemihyaline impact melt rock from Dellen, Sweden (DEL-01), and crystalline impact melt rock samples from Lappajärvi, Finland (LAP-01), Mistastin (LM-112-73), West Clearwater Lake (DCW-77-37-2), and Manicouagan (MANI-01), Canada, as well as samples from the Chicxulub impact crater that will be reported at LPSC 50.

Methods: For a single mineral phase there is a negative and linear correlation between crystal size and the natural log of the number of crystals present within individual size intervals [2,4]. Deviations from the linear trend indicate changes in the nucleation and/or crystallization relationships occurring as the crystallizing body cools [4]. As outlined in [2], it has been shown that there is a relationship between the slope of a CSD plot and its intercept that fundamentally defines how a body crystallizes [2]. Since the traditional CSD method of tracing individual crystals manually is a slow and time-consuming process, an automation method has been developed and tested. Initial results of this program were presented at the 49th LPSC [5]. This study is the next step in utilizing this new method for the rapid generation of CSDs. These are calculated by algorithmically isolating the crystals on a high-resolution image via a combination of color threshold filters from cross-polarized petrographic images. Binary masks are generated from the image using both Red-Green-Blue (RGB) and Hue-Saturation-Value (HSV) thresholds. Filtering via both of these standard color representation models allows for a more reliable isolation of crystals within the image. RGB is best suited to isolate crystal color and HSV can be more easily applied to crystal luminosity. Additionally, a light convolve effect is applied to each mask to filter out visual static, and the two masks are overlaid to generate a black-and-white trace of every crystal of a given phase in the sample. A custom user interface (UI) was written in Python using the OpenCV library to apply the filter

pipeline. This UI additionally allowed the filter thresholds to be calibrated for different mineral phases and makes the generation of output traces significantly faster. These traces are then processed in *ImageJ*, a free pixel analysis software [6]. *ImageJ* applies a best-fit ellipse to each crystal to determine a major and minor axis. Major and minor axes of the crystals are then exported to *CSDSlice* [7] and all data to *CSDCorrections* [8]. The former determines the approximate shape (e.g. rounded, oval, tabular, etc.) of the 2D traced crystals in three dimensions, and the latter sorts the crystals based on the length of the major axes and plots these in size bins based on the number of crystals present versus the natural log (ln) of the population phase.

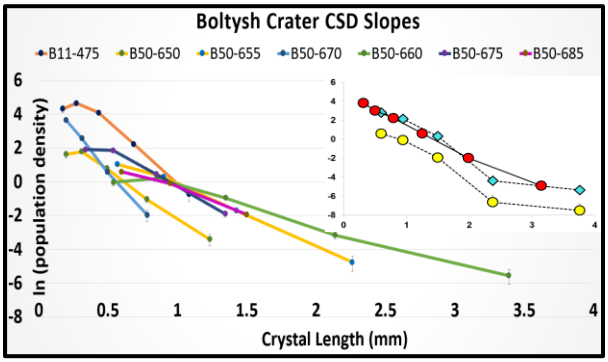

Figure 2: *Plotted CSDs for Boltysh samples studied. Inset: CSD Profile comparison of the new automated method* ***(red)*** *and the manual method* ***(yellow)*** *of the same sample (B50-685). For a given CSD slope, population density has a positive correlation with the intercept. When manual crystal count is proportionally increased* ***(cyan)*** *to the crystal count of the automated method, it is statistically similar [5].*

Results and Discussion: The CSDs produced by this automated method can be seen in **Fig 2.** and are based on crystal populations that are above the 250 crystals statistical significance threshold. The slope and y-intercept of these CSDs can be seen in **Fig 3**. These data are calculated using only crystals that are >0.3 mm in length (as per [4]) as smaller size bins have a reduced population due to a loss in visual resolution of the image (**Fig 2**). For Boltysh samples, seven CSDs were generated using plagioclase and plotted (**Fig. 2**). Relative to lunar CSDs, the automated terrestrial impacts have comparable slopes but variation in the intercepts (**Fig. 3**). This shows that terrestrial samples display smaller and more crystals than Apollo impacts melts **(Fig.3)**. The microcrystalline Boltysh samples fall in the lower right, while the glassy samples are higher and to the left of the impact field **(Fig.3)**. This slope vs. intercept relationship is well constrained between lunar endogenous flows and impact melts (**Fig 3**). Although CSDs have been applied to terrestrial endogenous flows and interpreted with respect to magma chamber processes, the effects of impacts are undefined. These data show that terrestrial impacts fall in a field outside of lunar impacts. While this may represent differences in plagioclase nucleation and growth between the two planetary bodies, parameters such as sample composition, cooling rate, and volatile content should also be considered. However, as additional data is added this may change.

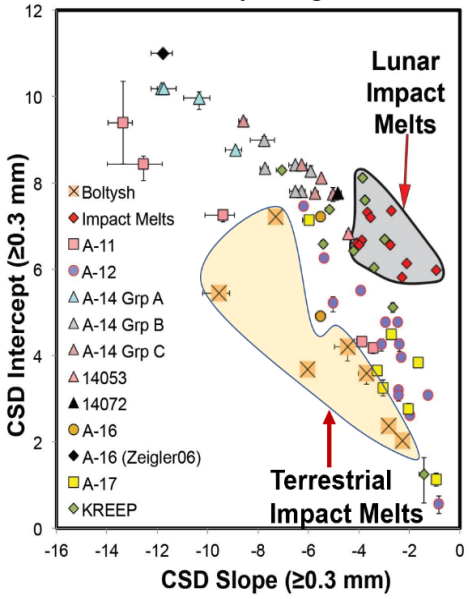

Figure 3: *Plotted CSDs for both lunar and terrestrial samples. Apollo data adapted from [4].*

Conclusions: These CSDs offer a direct comparison of the nucleation and growth habits of plagioclase in terrestrial and lunar impact melts. The terrestrial impact CSDs are distinct from the lunar impact field which suggests unique plagioclase growth between the two bodies. Future work will involve refining the terrestrial impact melt CSD field in **Fig. 3** which will involve expanding the number and variety of terrestrial impacts studied. This automated method will allow for rapid addition to the current terrestrial impact database.

A proven benefit of CSDs is that they are a non-destructive method of quantifying textures present in a rock. In the case of lunar samples this can define an endogenous flow from an impact melt and does not destroy valuable lunar material in the process.

Acknowledgement: We thank M. Schmieder (LPI) for providing impact melt samples from Australia, Sweden, Finland, and Canada.

References: [1] Neal C.R. et al. (2015) *GCA 148*, 62-80. [2] Marsh B.D. (1998) *J. Pet. 39*, 553-599. [3] Grieve R.A.F. et al. (1987) *Contrib. Mineral Petrol 96*, 56–62. [4] Higgins M.D. et al. (2006) *JVGR 154*, 8-16. [5] O'Brien H.C. et al. (2018) *LPS XLIX* Abstract #1534. [6] Schneider C. A. et al. (2012) *Nature Methods 9*, 671–675. [7] Morgan D.J., and Jerram D. A. (2006) *JVGR 154*, 1-7. [8] Higgins M.D. (2000) *Amer. Min. 85*, 1105-1116.